The EMBO Journal Vol.18 No.16 pp.4464–4475, 1999

Wrapping of DNA around the *E.coli* RNA polymerase open promoter complex

Claudio Rivetti[1], Martin Guthold[2] and Carlos Bustamante[1,3]

Istituto di Scienze Biochimiche, Università di Parma, 43100 Parma, Italy, [2]Computer Science Department, Department of Physics and Astronomy, University of North Carolina, Chapel Hill, NC 27599-3255 and [3]Departments of Physics and Molecular Cell Biology, University of California, Berkeley, CA 94720-7300, USA

[1]Corresponding authors
e-mail: rivetti@unipr.it

High-resolution atomic force microscopy (AFM) and biochemical methods were used to analyze the structure of *Escherichia coli* RNA polymerase·σ^{70} (RNAP) open promoter complex (RP_o). A detailed analysis of a large number of molecules shows that the DNA contour length of RP_o is reduced by ~30 nm (~90 bp) relative to the free DNA. The DNA bend angle measured with different methods varied from 55 to 88°. The contour length reduction and the DNA bend angle were much less in inactive RNAP–DNA complexes. These results, together with previously published observations, strongly support the notion that during transcription initiation, the promoter DNA wraps nearly 300° around the polymerase. This amount of DNA bending requires an energy of 60 kJ/mol. The structural analysis of the open promoter complexes revealed that two-thirds of the DNA wrapped around the RNAP is part of a region upstream of the transcription start site, whereas the remaining one-third is part of the downstream region. Based on these data, a model of the σ^{70}·RP_o conformation is proposed.

Keywords: atomic force microscopy (AFM)/DNA bending/DNA wrapping/open promoter complex/RNA polymerase/transcription

Introduction

Transcription initiation in *Escherichia coli* is characterized by the binding of RNA polymerase (RNAP) to the promoter DNA, followed by a sequence of conformational changes, involving both the DNA and the protein, that result in partial strand separation and formation of the open promoter complex (RP_o) (von Hippel *et al*., 1984; Leirmo and Record, 1990; Shu and Record, 1993). A variety of techniques have been used to analyze the structure of the RP_o complex and other intermediates of the reaction. The structure of *E.coli* RNAP, obtained by electron crystallography at ~25 Å resolution, revealed an overall size of the enzyme of ~100×100×160 Å and the presence of a channel 25 Å in diameter and 55 Å in length that has been proposed to comprise the DNA-binding site (Darst *et al*., 1989; Polyakov *et al*., 1995). Many DNase I and hydroxyradical DNA footprinting studies of the σ^{70} RP_o have shown that a DNA length of ~70–95 bp (240–320 Å) is protected from cleavage (Schickor *et al*., 1990; Craig *et al*., 1995). The extent of this DNA protection largely exceeds the length of the putative DNA-binding channel and is even more extended than the longest axis of the RNAP.

Several studies have also investigated the DNA bend angle induced by RNAP upon promoter binding. Gel mobility analysis of *E.coli* RNAP bound to the A1 promoter of the phage T7 has shown a lower mobility of complexes bound near the center of the DNA fragment compared with those bound close to the ends (Heumann *et al*., 1988b). A neutron scattering study of this complex has determined a DNA bend angle of $<45°$ (Heumann *et al*., 1988a) and, successively, quantitative electro-optics has estimated a value of $45 \pm 5°$ for the bend angle induced by RNAP (Meyer-Alme *et al*., 1994). Furthermore, circular permutation analysis has also demonstrated RNAP-induced bending at the *gal* promoter (Kuhnke *et al*., 1989). Electron microscopy studies of RNAP complexes with the T7 promoter showed the DNA bent (Williams and Chamberlin, 1977), but these data were not analyzed statistically. A more accurate analysis of DNA bend angle induced by RNAP has been presented in two atomic force microscopy (AFM) studies. In the first, σ^{70} RP_o at the λP_L promoter showed a bend angle distribution centered around 54° (Rees *et al*., 1993). In a similar work, AFM images of σ^{54} RP_o at the *glnA* promoter showed a distribution of bend angles centered around 114°. In addition, the contour length of DNA fragments containing the RNAP·σ^{54}–DNA open complex was significantly shorter than that of free DNA molecules, indicating a possible wrapping of the DNA around the RNAP (Rippe *et al*., 1997).

Other authors previously have suggested that in the initiation complex the DNA may wrap around the surface of the polymerase forming a nucleosome-like structure. Evidence for DNA wrapping has emerged from DNA supercoiling experiments (Amouyal and Buc, 1987), DNA footprinting (Schickor *et al*., 1990; Craig *et al*., 1995; Nickerson and Achberger, 1995), protein–DNA cross-linking and microscopy analysis (Polyakov *et al*., 1995; Kim *et al*., 1997; Rippe *et al*., 1997; Robert *et al*., 1998).

To understand further the process of transcription initiation, we have investigated the structure of *E.coli* RNAP·σ^{70} open promoter complex formed at the λ_{PR} promoter using a combination of biochemical and AFM methods. Taking advantage of the high resolution and contrast that can be obtained with AFM (Bustamante *et al*., 1993, 1997; Bustamante and Rivetti, 1996), DNA contour length and DNA bend angle analyses were performed on a large number of RNAP–DNA complexes. The results presented here provide strong evidence that

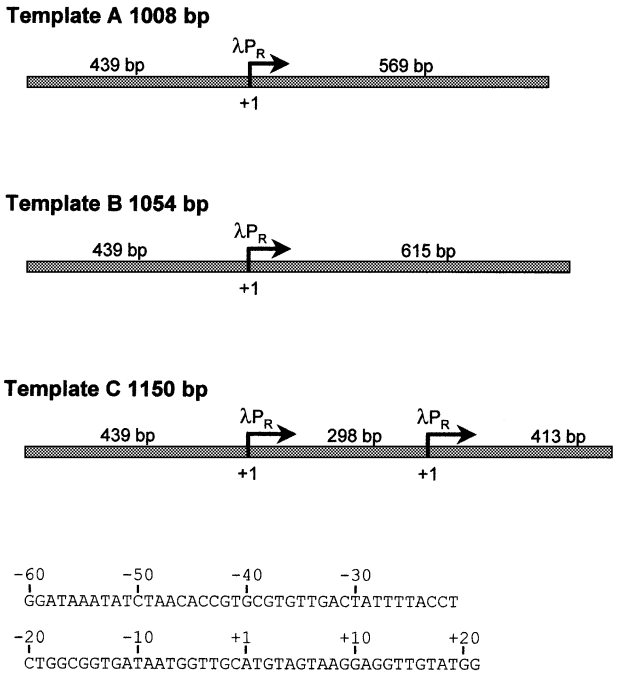

Fig. 1. Schematic representation of the three DNA templates and sequence of the λ_{PR} promoter used in this study. The transcription start site (+1) is used as the promoter reference point, and the direction of transcription is indicated by an arrow.

DNA wraps around the RNAP open promoter complex. Possible implications of the effect of Ni^{2+} ions, which have been used to enhance adsorption of DNA and protein–DNA complexes onto mica (Hansma *et al*., 1995, 1996; Kasas *et al*., 1997; Schulz *et al*., 1998), on the conformation of open promoter complexes are also discussed.

Results

Images of RNAP–DNA complexes

Three different DNA templates (denoted as A, B and C) were used to study the conformation of *E.coli* RNAP open promoter complexes by AFM (Figure 1). All DNA templates contain one or two λ_{PR} promoters located near the center of the molecule. Templates A and B were designed such that the short arm corresponds to the upstream and the long arm corresponds to the downstream region of the promoter. A typical image of RP_o assembled with template B (1054 bp) is shown in Figure 2A. Under these conditions, most of the DNA molecules have one RNAP bound and the concentration of complexes on the surface is ideal for DNA bend angle and contour length measurements. The activity of open promoter complexes was verified by *in vitro* transcription assays as described in Materials and methods. Figure 2B depicts open promoter complexes formed with template C (1150 bp) which contains two λ_{PR} promoters separated by 298 bp. Conditions were found in which one or both promoters were occupied by an RNAP. Usually ~50% of the DNA molecules in the image had a single RNAP bound, ~30% had two RNAPs bound and ~20% were free of proteins. In this case, because of the position of the two promoters relative to the DNA ends, it was not possible to determine whether RNAP had bound to the first or the second promoter.

Figure 2C shows DNA molecules of template C alone, with one and with two polymerases bound. The thin black lines represent the DNA contour traced as described in Materials and methods. The contour length of each trace is indicated in the image. The small dots are the nearest point along the contour to the center of the RNAP. The thick blue lines are the segments drawn to measure the DNA bend angles.

Figure 2D is an image of complexes between RNAP and template B that were obtained in the presence of a sufficiently high concentration of the transcription inhibitor heparin that competes for the DNA-binding site of RNAP (Schlax *et al*., 1995). Under these conditions, it was observed that RNAP can, to some degree, still bind to the DNA and appears to have a higher affinity for the DNA ends. *In vitro* transcription assay showed that these heparin-resistant complexes are not transcriptionally active (data not shown). Presumably, these complexes involve the binding of RNAP through some type of non-specific interaction. This interpretation is supported by the random distribution of the RNAP bound along the DNA. To increase the number of complexes on the surface, the reaction was carried out using a higher protein concentration. These complexes will be used as controls in the analysis that follows.

Position of the RNAP along the template DNA

The position of the RNAP along the DNA template was determined by measuring the DNA contour length from the center of the RNAP to each end. The position was then expressed as the ratio between the shorter and the longer arm of the DNA. Table I compares the expected arm ratios, calculated from the DNA sequence assuming the transcription start site to be at the center of the RNAP, with the arm ratios measured from the AFM images. Interestingly, all complexes analyzed displayed an arm ratio smaller than that expected from the DNA sequence. This result indicates that the transcription start site does not coincide with the center of the RNAP. Significantly, DNA footprinting experiments showed that of the 95 bp protected by the polymerase, 70 bp are upstream and 25 bp downstream of the transcription start site (Craig *et al*., 1995). A more accurate analysis of the contour length of the DNA arms is reported below.

The arm ratio was used to exclude non-specific complexes from the analysis. In the case of templates A and B, only those complexes in which the arm ratio was within one standard deviation from the mean were considered. The same procedure was used to select complexes of template C with one RNAP bound since the expected arm ratio for binding at either promoter was very similar (Table I). No selection procedures were applied to complexes on template C with two RNAPs bound.

The asymmetric location of the RNAP makes it possible also to determine the orientation of the complexes on the surface. This was done by analyzing the direction of bending of the downstream DNA with respect to the upstream DNA. Table II shows that complexes with the bend towards the left and those with the bend towards the right are equally populated. Thus, His_6-RNAP does not produce a preferential binding of the complexes to the

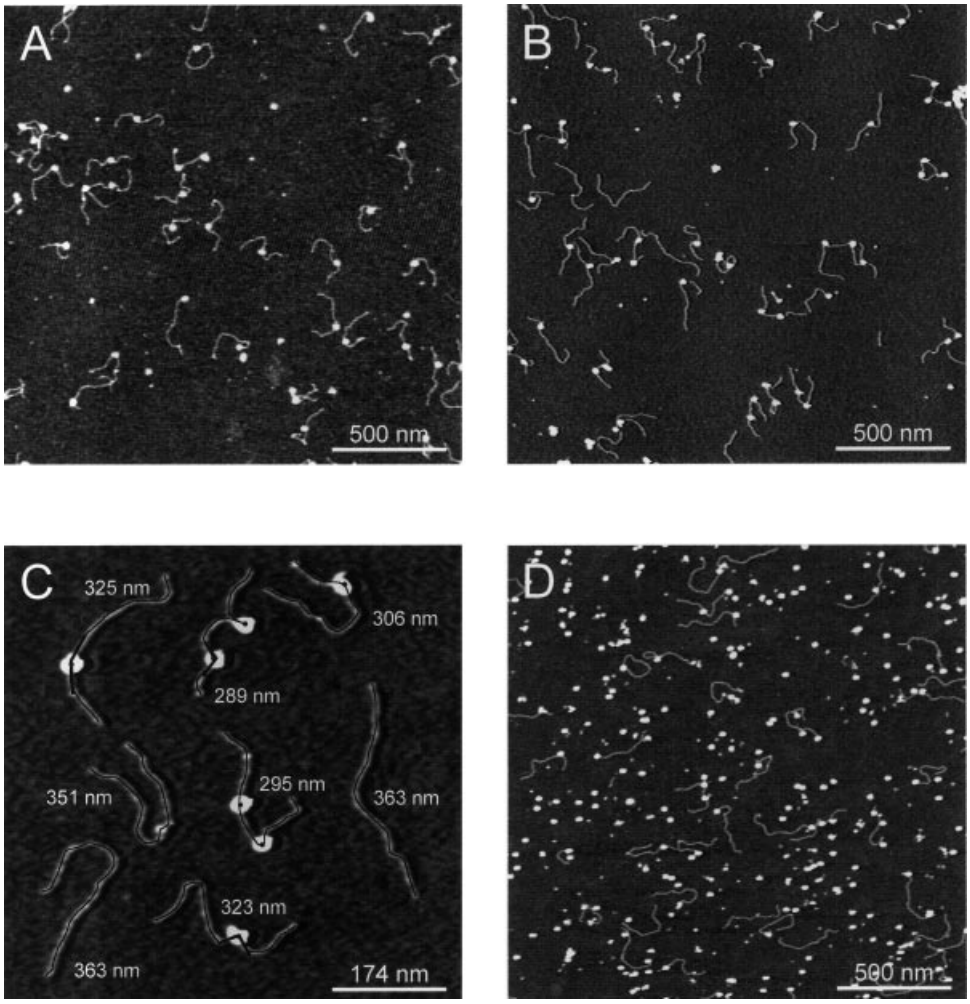

Fig. 2. Atomic force microscopy images of RNAP–DNA complexes. The RNAP molecules are seen as white dots. (**A**) Image of RP_o on template B. (**B**) Image of RP_o on template C. In this image, some DNA molecules have no protein bound, some DNA molecules have one RP_o and some DNA molecules have two RP_os. (**C**) Close up of an image as in (B). Also visualized are the DNA contour (thin black lines) traced as described in Materials and methods, the position of the RNAP (small black dots) and the tangents drawn to measure the DNA bend angle (thick black lines). The values in nanometers are the DNA contour length measure for each molecule. (**D**) Image of RNAP–DNA complexes assembled in the presence of heparin. The larger number of polymerases with respect to DNA molecules reflect a higher concentration of RNAP used to make these complexes. All images were recorded in air with the microscope operating in tapping mode. The color code corresponds to a height range of 5 nm from dark to clear.

mica surface even in the presence of $NiSO_4$. This result differ from data published previously where mostly left-handed configurations were observed in AFM images of His_6-RNAP complexes (Hansma *et al*., 1997).

DNA bend angle measurements

As shown in Figure 2A–C, the DNA of *E.coli* RNAP open promoter complexes appears bent by the binding of the polymerase. To quantify the extent of protein-induced DNA bending, we have employed AFM imaging and polyacrylamide gel electrophoresis. Measurements of DNA bend angles from the AFM images were performed using the tangents method and the mean square end-to-end distance method (Materials and methods).

The bend angle distributions of open promoter complexes obtained with the tangents method are shown in Figure 3. For each distribution, the mean value and the standard deviation of the Gaussian fitting are summarized in Table II. The bend angle of RP_o formed with template A, B or C, in this latter case considering only those complexes with one RNAP bound (Figure 3A–C), is ~60°. The distributions are very broad, with a standard deviation around ±60°. A single Gaussian curve was used to fit

Table I. DNA arm ratios of *E.coli* RNAP open promoter complexes

	Expected	Measured	No. of complexes
RP_o (A)	0.77	0.70 ± 0.08	514
RP_o (B)	0.71	0.67 ± 0.08	560
RP_o (C)	0.57 or 0.60	0.55 ± 0.06	157
RP_o (B) 5 mM $NiSO_4$	0.71	0.67 ± 0.04	223
RP_o (B) 15 mM $NiSO_4$	0.71	0.69 ± 0.05	209

The expected values were determined from the ratio between the shorter and the longer DNA regions relative to the transcription start site. The two values reported for RP_o with template C refer to the two promoters present in this DNA fragment. The measured values were obtained from the ratio of the shorter and the longer arm of the DNA relative to the center of the RNAP. The letters in parentheses indicate the DNA template used.

Table II. DNA bend angle of *E.coli* RNAP open promoter complexes

	AFM tangents	Bend direction		AFM $\langle R^2 \rangle$	Gel mobility		No. of complexes
		Left	Right		14° A-tract	18° A-tract	
RP_o (A)	55 ± 55°	45%	55%	70°	74 ± 1°	58 ± 1°	514
RP_o (B)	56 ± 54°	59%	41%	73°	81 ± 1°	63 ± 1°	560
RP_o (C)	61 ± 75°			88°	–	–	157
Two RP_os (C)	40 ± 67°			–	–	–	173
RP_o (B) 5 mM $NiSO_4$	21 ± 62°	52%	48%	19°	–	–	223
RP_o (B) 15 mM $NiSO_4$	13 ± 53°	47%	53%	0°	–	–	209

Bend angle values determined with the tangents method are the mean of the Gaussian fit of the bend angle distributions (Figure 3) ± the standard deviation from the mean. Bend angle values obtained from the $\langle R^2 \rangle$ were calculated using Equation 1. In gel mobility assays, the bend angle was determined from calibration curves of A-tract markers assuming either 14 or 18° bending for each A-tract. The values are the mean ± SD of three independent experiments. The number of complexes corresponds to those analyzed with AFM methods. The letters in parentheses indicate the DNA template used.

the bend angle distributions because previous $KMnO_4$ footprinting experiments indicate that, under the present conditions, RNAP·σ^{70} complexes at the λ_{PR} promoter exist predominantly in a well defined, single open promoter configuration (Tsodikov *et al*., 1998), whereas other configurations, such as closed promoter complexes or intermediate complexes, are not significantly populated.

The distribution in Figure 3D corresponds to all the bend angles measured from template C with two RNAPs bound. The mean of the Gaussian fitting to this distribution is 40 ± 67°. This value is lower than the value of 60° obtained for the two single promoters. A lower value would be expected in the case where the two bends do not lie in the same plane. This implies a distortion of one or both angles during the transition from three to two dimensions upon deposition onto the mica surface. The distance between the two promoters is 298 bp, which corresponds to 298/10.5 = 28.4 DNA turns. Moreover, the exact value of the dihedral angle between the two RP_os will also be influenced by the DNA unwinding of the DNA region at each promoter. With the mean square end-to-end distance method, a bend angle of ~70° was determined for templates A and B and 88° for template C (Table II).

Gel mobility assays were performed with RP_o on template A or B. In the absence of polymerase, these DNA fragments displayed the same gel mobility, indicating the absence of intrinsic bending. Conversely, a significant lower mobility of the 'middle' RP_o with respect to the 'end' RP_o was observed. Table II reports the bend angles measured from gel mobility assay, using calibration curves obtained with a set of DNA fragments harboring phased A-tracts (Thompson and Landy, 1988).

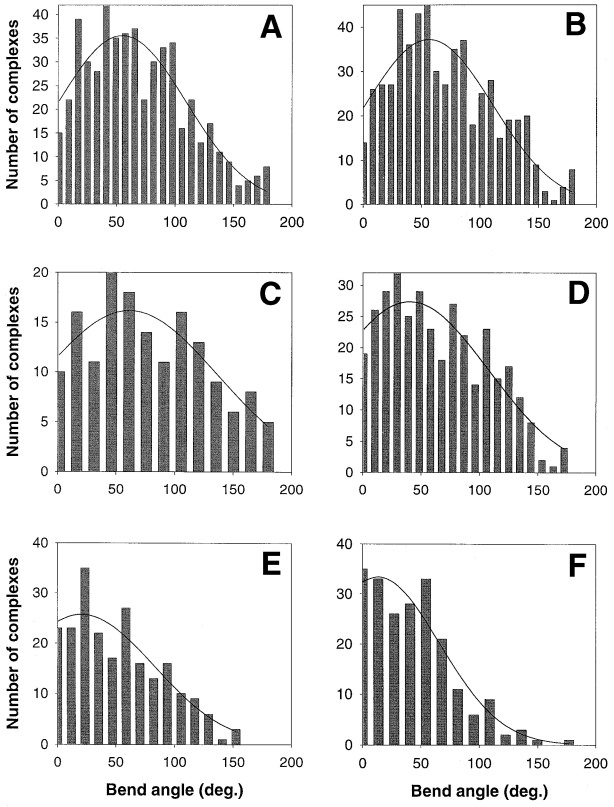

Fig. 3. DNA bend angle distributions of open promoter complexes determined with the tangents method. In all cases, the number of classes is the square root of the number of complexes. The lines represent the Gaussian fitting of the distribution, and the values obtained from the fitting are reported in Table II. (**A**) RP_o with template A. (**B**) RP_o with template B. (**C**) A single RP_o on template C. (**D**) Two RP_os on template C. In this latter case, the two complexes could not be discriminated, therefore, their bend angles were pulled into a single distribution. (**E**) RP_o with template B exposed to 5 mM $NiSO_4$. (**F**) RP_o with template B exposed to 15 mM $NiSO_4$.

DNA contour length analysis

A structural feature that can be measured easily from the AFM images of DNA and open promoter complexes is the DNA contour length. This measurement is done by tracing the DNA backbone from one end to the other and calculating the length of the traced line. In the case of DNA alone, the whole molecule is visible and the procedure is straightforward. On the other hand, when imaging protein–DNA complexes, the DNA that is in contact with or in close proximity to the RNAP is hidden by the broadening effect of the tip. Therefore, contour length measurements of RP_o assume that the DNA passes through the center of the protein. If this was the case, i.e. if the RNAP simply sits astride the DNA, little or no difference should be observed between the contour length of free DNA molecules and those in RP_o.

In order to compare data from different experiments,

particular care was taken for those experimental parameters that could bias the measurements. In particular, all the images were collected with equal scan size and all sample depositions were done in the same buffer conditions using ruby mica as a substrate. All the DNA contour length measurements were carried out with the same procedure by the same user. When possible, molecules of free DNA and RP_o were measured from the same set of images.

DNA molecules

The contour length distributions of the three DNA fragments (A, B and C) used for this study are shown in Figure 4, and the mean values, given by the Gaussian fitting of these distributions, are reported in Table III. The DNA rise per base pair, as determined from the ratio of the measured contour length of DNA and the number of base pairs for each DNA fragment, is 3.2 Å/bp. This value is slightly smaller than the canonical value of 3.4 Å/bp for B-form DNA. The discrepancy is probably due to the smoothing routine applied to the DNA trace to reduce the noise and to the limited resolution of the microscope.

Using the DNA contour length and the $\langle R^2 \rangle$, it is possible to determine the DNA persistence length from images of free DNA molecules (Frontali *et al*., 1979; Rivetti *et al*., 1996). From all the DNA templates used, a persistence length of ~50 nm was calculated. This value is in agreement with previously reported data and with previous results showing that the deposition process does not alter the conformation of the molecules (Rivetti *et al*., 1996). The fact that the $\langle R^2 \rangle$ value is close to the value expected for intrinsically straight polymers in two dimensions also suggests the absence of intrinsic bends or kinks in DNA fragments containing one or two λP_R promoters. This interpretation is supported by the absence of a band shift in gel mobility experiments of promoter DNA without polymerase. Alternatively, the bend may be either too small to influence the $\langle R^2 \rangle$ significantly or, less likely, the effect produced by a bend may be counterbalanced exactly by an opposite bend or by a higher persistence length of the DNA.

Open promoter complexes

Figure 4A shows the distributions of the contour length measurements obtained with template A alone and in RP_o. The mean values, given by the Gaussian fitting of these distributions, are reported in Table III. A significant shift toward lower values of the center of the contour length distribution for RP_o can be seen. The contour length reduction, expressed in terms of the difference between the mean values of the two distributions, is 32 nm. The DNA contour length measurements of RP_o on template B (Figure 4B; Table III) showed a reduction of 28 nm with respect to the free DNA. The contour length distributions, obtained with template C alone and in complex with one or two polymerases, are shown in Figure 4C. In this case, the reduction observed for complexes with one polymerase bound was 31 nm (Table III). Interestingly, when both promoters were occupied by an RNAP, the contour length reduction was 55 nm, almost twice that observed with one RP_o. In this experiment, free DNA molecules and open promoter complexes were measured from the same set of images. To increase the number of DNA molecules evaluated, some measurements were also done on a separate set of images of free DNA. No difference in the mean contour length of free DNA molecules was observed between the two experiments.

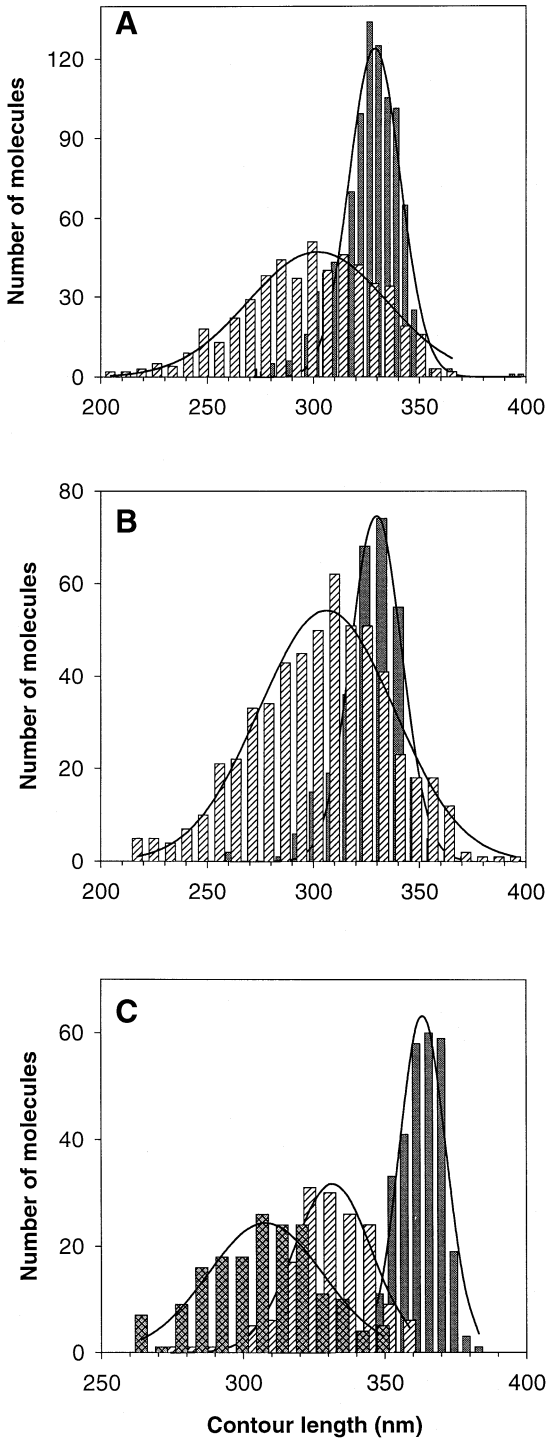

Fig. 4. Contour length distributions of free DNA molecules and open promoter complexes. In all panels, the number of classes was determined by the square root of the number of complexes. The lines represent the Gaussian fitting of the distribution, and the values obtained from the fitting are reported in Table III. (**A**) Free DNA molecules of template A (filled gray bars) and RP_o with template A (hatched bars). (**B**) Free DNA molecules of template B (filled gray bars) and RP_o with template B (hatched bars). (**C**) Free DNA molecules of template C (filled gray bars), one RP_o on template C (hatched bars) and two RP_os on template C (crossed-hatched bars).

Table III. Contour length of free DNA molecules and *E.coli* RNAP–DNA complexes

	Contour length (Gaussian fit) (nm)	Difference from free DNA (nm)	No. of molecules
DNA (A)	329 ± 12		947
RP_o (A)	297 ± 34	32	514
DNA (B)	330 ± 13		302
RP_o (B)	302 ± 34	28	560
DNA (C)	363 ± 8		317
One RP_o (C)	332 ± 14	31	157
Two RP_os (C)	308 ± 20	55	173
DNA (B) 5 mM $NiSO_4$	322 ± 12		315
RP_o (B) 5 mM $NiSO_4$	303 ± 16	19	223
DNA (B) 15 mM $NiSO_4$	325 ± 9		120
RP_o (B) 15 mM $NiSO_4$	314 ± 15	11	209
DNA (C)	363 ± 8		317
Artificial complexes (C)	363 ± 12	0	338
DNA (B)	330 ±13		302
One complex (B) with heparin	329 ± 20	1	221
Two complexes (B) with heparin	335 ± 22	–5	46

The DNA contour length values are the mean of the Gaussian fit of the distributions reported in Figures 4, 6 and 7 ± the standard deviation from the mean. The difference from free DNA is the contour length of free DNA molecules minus the contour length of RNAP–DNA complexes. The letter in parentheses indicates the DNA template used.

The above results show that the formation of one RP_o on a DNA fragment causes a reduction of the DNA contour length of ~30 nm (~90 bp). As determined by electron crystallography, the *E.coli* RNAP is a globular feature with a circumference of ~32 nm (Darst *et al*., 1989). Therefore, the observed reduction of the DNA contour length is consistent with a model in which the DNA is actually wrapped around the protein surface. In some cases, the particular orientation of the complexes on the surface and the especially good imaging conditions gave rise to images in which a nucleosome-like structure of the RP_o was discernible. A gallery of such complexes is shown in Figure 5.

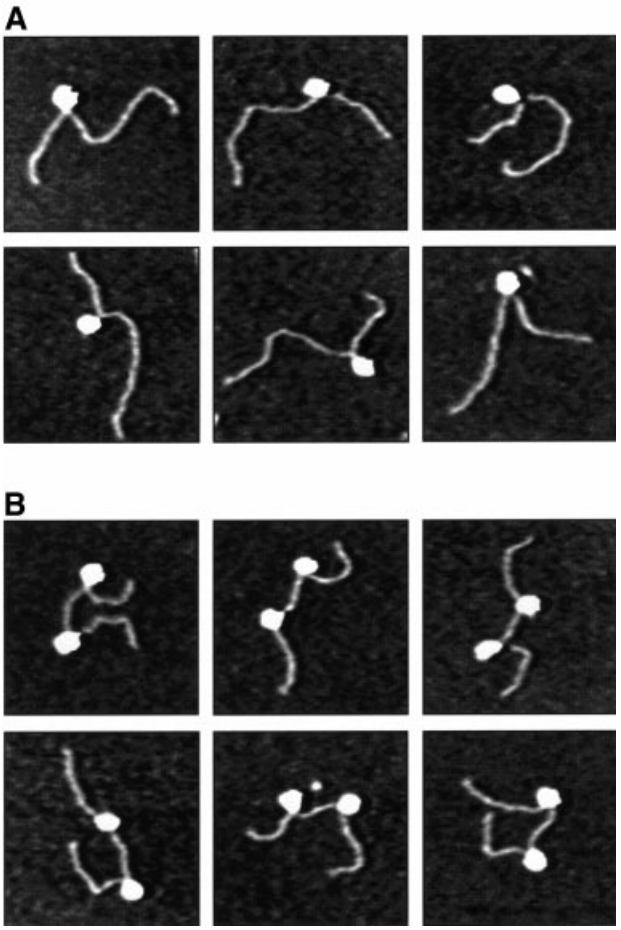

Fig. 5. Montage of AFM images showing open promoter complexes on template C. (**A**) The RNAP is bound to one promoter. (**B**) The RNAP is bound to both promoters. The shape of these complexes suggests a structure in which the DNA is wrapped around the polymerase. Image size: 250 nm. The images were recorded in air with the tapping mode. The color code corresponds to a height range of 5 nm from dark to clear.

Open promoter complexes in the presence of $NiSO_4$

Millimolar concentrations of $NiSO_4$ have been used to enhance adsorption of DNA and protein–DNA complexes onto mica in some previous AFM studies (Hansma *et al*., 1995, 1996; Kasas *et al*., 1997; Schulz *et al*., 1998). We found that the presence of millimolar concentrations of $NiSO_4$ in the *in vitro* transcription reaction completely inhibits RNA synthesis (data not shown). Complexes assembled with template B in conditions that favor RP_o formation were exposed to 5 or 10 mM $NiSO_4$, deposited on mica and imaged in air by AFM. The bend angle distributions obtained with the tangents method are shown in Figure 3E and F, and the values of the Gaussian fitting are reported in Table II. The presence of Ni^{2+} dramatically influences the DNA bend angle induced by the RNAP; at a concentration of 15 mM $NiSO_4$, the average bend angle is closed to 0°. This behavior is confirmed by the bend angle determination using the mean square end-to-end distance method. An inspection of the bend angle distributions in Figure 3A–D (active RP_o without $NiSO_4$) reveals that complexes with a bend angle close to zero are rare and that there are also several complexes with a bend angle of ~180° (i.e. RNAP is at the apex of a very sharp kink). The situation in the presence of $NiSO_4$ is reversed (Figure 3E and F): many complexes have a bend angle close to zero (i.e. the DNA is straight), and almost none have the sharp kink configuration seen before. In addition, these complexes showed a DNA contour length reduction of only 19 and 10 nm in 5 and 15 mM $NiSO_4$, respectively (Figure 6, Table III). It is interesting to observe that also in the presence of $NiSO_4$ the RNAP remains bound at the promoter as can be deduced from the arm ratio shown in Table I.

Artificial complexes and heparin-resistant complexes

Two control experiments were performed to validate further the measurements obtained from AFM images of RP_o complexes. The first type of experiment was designed to test if the presence of a globular feature along the DNA path could have biased the performance of the tracing routine used to measure the DNA contour length. To this

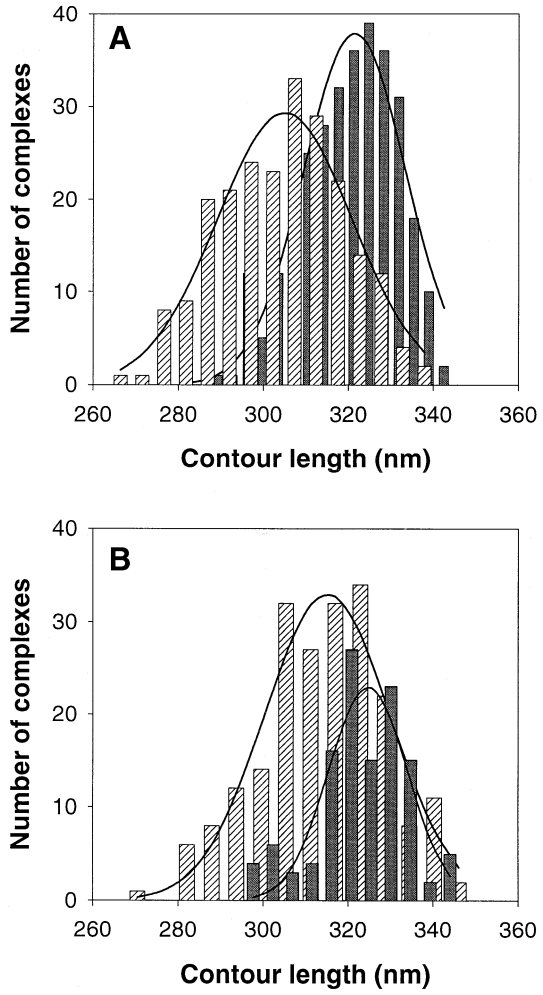

Fig. 6. DNA contour length distributions of open promoter complexes exposed to $NiSO_4$. The number of classes was determined by the square root of the number of complexes. The lines represent the Gaussian fitting of the distribution, and the values obtained from the fitting are reported in Table III. (**A**) Free DNA molecules of template B (filled gray bars) and RP_o in the presence of 5 mM $NiSO_4$ (hatched bars). (**B**) Free DNA molecules of template B (filled gray bars) and RP_o in the presence of 15 mM $NiSO_4$ (hatched bars).

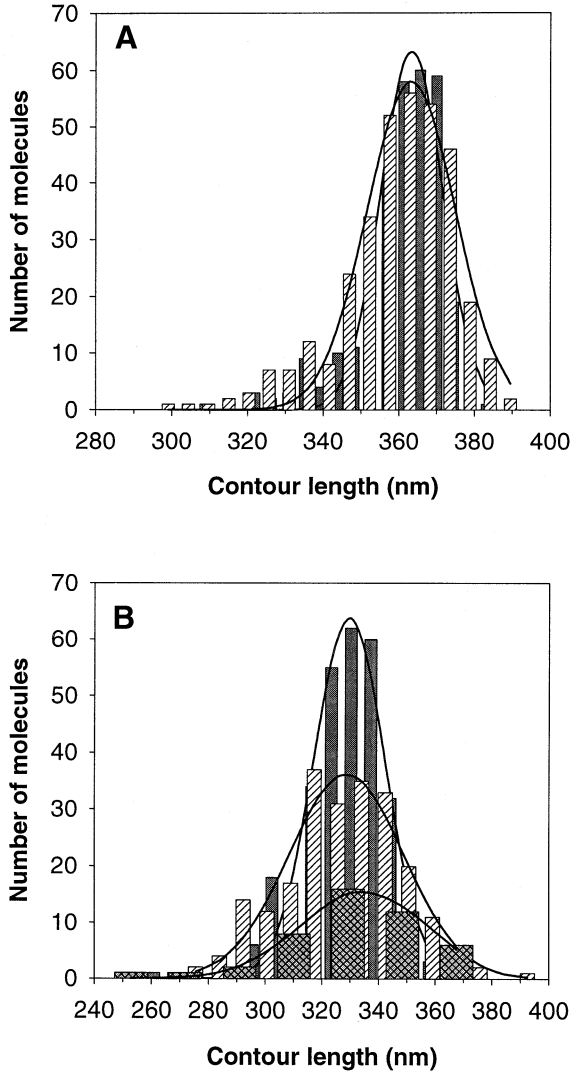

Fig. 7. DNA contour length distributions of the control experiments. The number of classes was determined by the square root of the number of complexes. The lines represent the Gaussian fitting of the distribution, and the values obtained from the fitting are reported in Table III. (**A**) Free DNA molecules of template C (filled gray bars) and artificial complexes (hatched bars) created as described in the text. (**B**) Free DNA molecules of template B (filled gray bars), template B with one heparin-resistant complex (hatched bars) and template B with two heparin-resistant complexes (crossed-hatched bars).

end, a set of images of DNA molecules was analyzed and the mean contour length was determined. Next, using software tools, the globular feature of an RNAP was superimposed on each DNA molecule to simulate an RNAP–DNA complex. Such artificial complexes were then re-measured and analyzed with the same procedure used for the free DNA. The contour length distributions obtained in the two cases (Figure 7A, Table III) were almost identical, arguing that no artifacts were introduced in the contour length measurement by a globular feature along the DNA path.

A second control was designed to determine whether non-specifically bound RNAP induces significant changes in the DNA contour length. This test is difficult to design because even a promoter-less DNA fragment could contain sequences that function as pseudo-specific binding sites for RNAP (Kadesch *et al.*, 1980). A way to overcome this problem is to form non-specific complexes in the presence of heparin. Heparin is a polyanion that mimics DNA and presumably inhibits transcription by interfering with the formation of a specific RNAP–DNA complex at the promoter. Therefore, the complexes observed in the presence of heparin are of a non-specific nature (Figure 2D). The analysis of these complexes shows that the presence of one or even two polymerases bound to the DNA in the presence of heparin does not reduce the DNA contour length (Figure 7B, Table III). DNA molecules with RNAP bound to one or both ends were not scored since the DNA contour length could not be measured accurately. In this experiment, all molecules were measured from the same set of images. These experiments indicate that the DNA contour length reduction observed in AFM measurements is a peculiar feature of active open promoter complexes.

Analysis of the DNA arms

The asymmetric location of the promoter within the DNA template makes it feasible to distinguish between the upstream and the downstream regions of the DNA with respect to the RNAP. It is possible, therefore, to determine the fraction of DNA wrapped around the polymerase that is part of the upstream or downstream arms of the template. Taking the transcription start site as the reference point, the expected arm ratio for template A is 0.77 (439/569). However, the ratio of the measured contour lengths of the upstream and downstream arms, obtained from the AFM images, was 0.70 (Table I). This smaller ratio is not due to the overall reduction in contour length of the RP_o. In fact, assuming an equivalent reduction for both DNA arms, the measured ratio would be:

$$\frac{439\ (\text{bp})\times 0.32\ (\text{nm/bp}) - 32/2\ (\text{nm})}{569\ (\text{bp})\times 0.32\ (\text{nm/bp}) - 32/2\ (\text{nm})} = 0.75$$

where 0.32 nm/bp is the rise per bp determined from the AFM images. Therefore, the experimentally observed value of 0.70 indicates that a larger portion of the upstream arm wraps around the polymerase than the downstream arm. The amount of upstream DNA (U_{DNA}) and downstream DNA ($32 - U_{DNA}$) wrapped around the polymerase can be obtained from the equation:

$$\frac{439\ (\text{bp})\times 0.32\ (\text{nm/bp}) - U_{DNA}\ (\text{nm})}{569\ (\text{bp})\times 0.32\ (\text{nm/bp}) - (32 - U_{DNA})\ (\text{nm})} = 0.70$$

from which a U_{DNA} value of 20 nm is obtained. Thus, approximately two-thirds (~60 bp) of the total DNA length wrapped around the RNAP in RP_o can be attributed to the upstream arm and one-third (~30 bp) to the downstream arm. Similar results are obtained with template B. This result is in agreement with footprinting (Craig *et al*., 1995) and cross-linking data (Brodolin *et al*., 1993), and with the high degree of conservation found in the –10 and –35 regions among prokaryotic promoters (Hawley and McClure, 1983).

Discussion

In this report, it has been shown that traditional biochemical methods combined with a detailed analysis of high resolution AFM images can provide new insights into the conformation of the *E.coli* transcription initiation complex. The data presented here confirm previous observations (Heumann *et al*., 1988b; Rees *et al*., 1993; Rippe *et al*., 1997) that upon RP_o formation, the binding of RNAP bends the promoter DNA. By using different methods, a DNA bend angle of ~60–70° was determined. The good correspondence between bend angle values obtained by gel retardation and those measured by AFM indicates that the three-dimensional conformation of the complexes in solution is maintained upon deposition onto the mica substrate. Moreover, it shows that the end-to-end distance method is a valuable alternative to the tangents method for bend angle determination. Although the tangent method has the advantage of giving not only the mean bend angle but also the bend angle distribution of a population of complexes, it is often difficult to estimate the exact location of the DNA exiting from the protein because of the broadening effect of the AFM tip. On the other hand, end-to-end distance measurements are influenced minimally by the broadening effect of the tip but they do not provide information on the distribution of bend angles. The bend angle distributions shown in Figure 3 are rather broad. This could reflect open promoter complexes with a well defined bend angle that are adsorbed onto the surface in slightly different orientations. In addition, thermal fluctuations will broaden the distributions to some extent. It may also be argued that the distributions are multi-modal and might reflect different configurations of the protein–DNA complex, such as closed or intermediate complexes. However, in light of evidence (Tsodikov *et al*., 1998) that σ^{70} RNAP at the λ_{PR} promoter forms exclusively open complexes under the present conditions, this latter interpretation has not been considered. This is different from σ^{54} RNAP where open complex formation is inefficient and open complexes coexist with a significant population of closed complexes (Rippe *et al*., 1997).

A second important result that has emerged from this study is that the DNA contour length of RP_o is 30 nm less than the contour length of protein-free DNA molecules. This result is indicative of DNA wrapping around the surface of the polymerase in the RP_o complex. Consequently, the overall DNA distortion is much larger than the apparent bend angle and is estimated to be ~300° (Figure 8A).

When open promoter complexes were exposed to millimolar concentrations of $NiSO_4$, the synthesis of RNA was prevented as demonstrated by *in vitro* transcription. The AFM analysis of such complexes has revealed that at 15 mM $NiSO_4$ the DNA bend angle induced by RNAP disappears and the contour length is reduced by only 10 nm. This effect cannot be attributed to the binding of the Ni^{2+} ions to the histidine tag of the β′ subunit because His_6-RNAP is active when bound to Ni^{2+}-NTA–agarose (Kashlev *et al*., 1993). In addition, *in vitro* transcription with wild-type RNAP gave similar results (Niyogi and Feldman, 1981).

Because of the limited amount of data in the literature, we can only present a speculative hypothesis to explain the observed Ni^{2+} effect upon transcription. As proposed by Craig *et al*. (1995), an Mg^{2+} ion on the RNAP located near position –38 could be responsible for the increased DNA bending that accompanies the formation of the RP_o. Such a bending is thought to be crucial for wrapping of the DNA around the polymerase. It is possible that the substitution of Mg^{2+} with Ni^{2+} causes loss of activity, the disappearance of the bend angle and unwrapping of the DNA from the polymerase. Alternatively, it is possible that millimolar concentrations of Ni^{2+} could make the polymerase adopt a closed complex conformation. This hypothesis would also explain the promoter localization of the polymerase in the presence of Ni^{2+} as observed from the images (Table I).

In the past, several authors have proposed the possibility that the DNA might wrap around the polymerase in the initiation complex. (i) DNA topology experiments of RP_o, with both weak and strong promoters, revealed that a strand separation of 12 bp could not account for the observed topological unwinding of 1.7 turns (Amouyal and Buc, 1987). Because the measured unwinding was

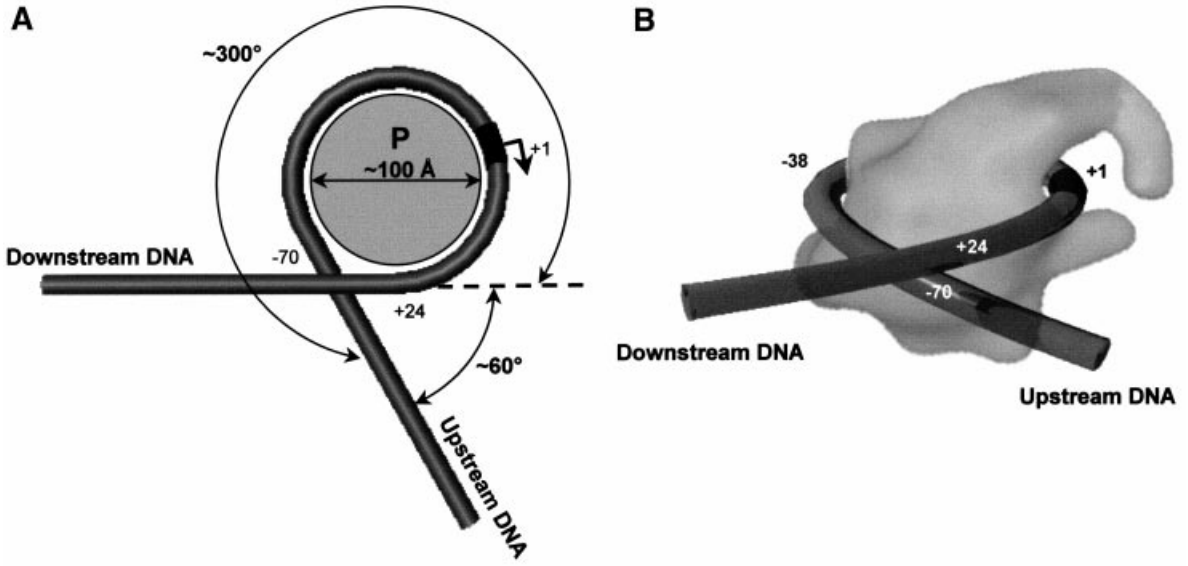

Fig. 8. Proposed model of the *E.coli* RNAP·σ^{70} open promoter complex. (**A**) Schematic view showing the RNAP in light gray and the trajectory of the DNA in dark gray. A bend angle of ~60° has been measured by AFM and gel retardation. A bend angle of ~300° is inferred when DNA wrapping is taken into account. The position of the start site (black patch) and the length of wrapping are consistent with the results presented in this work. (**B**) Three-dimensional representation of DNA wrapping around the polymerase. The RNAP holoenzyme was drawn according to Darst *et al*. (1989). The RNAP channel has been drawn closed as described in Polyakov *et al*. (1995). The trajectory of the DNA has been drawn in a left-handed superhelix configuration in agreement with topological experiments (Amouyal and Buc, 1987).

effectively a change in linking number, it was suggested that both untwisting and negative writhing contributed to the total unwinding. (ii) In DNA footprinting experiments, the length of DNA protection by RNAP (~30 nm or ~90 bp) was explained as evidence of DNA wrapping (Schickor *et al*., 1990; Craig *et al*., 1995). (iii) In addition, the cleavage pattern with a periodicity of ~11 bp, similar to that observed for nucleosomal DNA (Hayes *et al*., 1990), indicates that the RNAP contacts one side of the DNA helix. Since 5 bp out of 11 are protected, it was proposed that the DNA may lie in an extensive groove on the surface of the polymerase (Craig *et al*., 1995). The data presented here show that ~30 nm of DNA appear missing from the images of RP_os. This and previous observations are consistent with the idea that the DNA wraps around the polymerase. A model of the structure of *E.coli* RNAP·σ^{70} open promoter complex is drawn in Figure 8. In this model, the DNA wraps completely around the polymerase two-thirds involving the upstream and one-third the downstream DNA region. Consequently, the region of strand separation that occurs slightly upstream of the transcription start site is located near the cleft produced by a thumb-like structure, which has been suggested to contain the active center of RNAP (Darst *et al*., 1989; Polyakov *et al*., 1995). Complete wrapping of the DNA around the polymerase and crossing of the upstream and downstream arms have been invoked to reconcile the 30 nm reduction in DNA contour length with the 60–70° DNA bending measured from the images of RP_os. The handedness of the superhelix has been drawn according to topological experiments (Amouyal and Buc, 1987).

The identification of the UP element (a DNA sequence rich in A + T) in some bacterial promoters, located around bp –40 to –60, has expanded the region of DNA recognition by RNAP (Ross *et al*., 1993). The UP element makes specific contacts with the RNAP αCTD and can stimulate transcription up to 100-fold. This interaction is thought to participate in the wrapping of DNA around the RNAP. It must be mentioned that the DNA sequence upstream of the λ_{PR} promoter used in this study (Figure 1) did not show any significant similarity with the UP element. Therefore, it would be of interest to analyze the effects on wrapping of the removal of the αCTD and/or of substitutions within promoter upstream sequences.

DNA wrapping has also been proposed for the pre-initiation complex of eukaryotic RNAP II in three recent protein–DNA photo-cross-linking studies (Forget *et al*., 1997; Kim *et al*., 1997; Robert *et al*., 1998). Kim *et al*. and Forget *et al*. have based their hypotheses also on the observation that pre-initiation complexes imaged by electron microscopy showed a reduced DNA contour length of ~50 bp compared with protein-free DNA molecules. In these studies, it is also proposed that DNA wrapping in initiation complexes might be a common feature of all multi-subunit RNA polymerases.

Transcription is a process of fundamental importance for the cell. The stability of the transcription complex is affected by the extent of the protein–DNA interactions. DNA wrapping around the polymerase maximizes the contact area between the DNA and the polymerase while keeping the protein relatively small. In *E.coli*, the length of the DNA that is in contact with the RNAP (~30 nm) is twice as large as the longest axis of the protein (16 nm). A requirement for transcription initiation is that ~12 bp at the transcription start site are unwound and the two DNA strands are separated. A superhelical left-handed twist produced by wrapping of the DNA around the protein core provides the potential for the topological conversion of negative writhe into local untwisting (Wasserman *et al*., 1988).

It is of interest to estimate the bending energy required

to make the promoter DNA wrap around the polymerase. Assuming a uniform deformation around the surface of the protein, the energy to bend a worm-like chain of length l by an angle θ is given by

$$E_{\text{bend}} = \frac{Pk_BT\theta^2}{2l}$$

(Landau and Lifschitz, 1980, 1986), where P is the DNA persistence length, k_B is the Boltzmann constant and T is the absolute temperature. Assuming a persistence length of 53 nm (Rivetti *et al*., 1996), the formation of a 300° (5/3π) bend, extended over a length l of 30 nm, requires 60 kJ/mol. This energy may be less if the promoter region has a higher 'bendability' due to intrinsic bending, increased flexibility or the interaction of protein factors. Previously, it has been estimated that the free energy, ΔG, of the reaction $R + P \rightarrow RP_o$ at the λP_R promoter is –60 kJ/mol (at 25°C), from which an association constant of 3.2×10^{10}/M is determined (Roe *et al*., 1985). Thus, it appears that without the energy cost of DNA bending, the ΔG for RP_o formation would be around –120 kJ/mol. This energy would probably be too high to permit the escape of the polymerase from the promoter. Thus, the energy required for DNA bending may have the additional benefit of facilitating promoter clearance.

DNA wrapping around the polymerase in RP_o opens up a number of possible relevant interactions between the enzyme and specific sequences near the promoter. These interactions may play an important role during promoter recognition, promoter clearance and transcription regulation.

Materials and methods

Preparation of DNA and protein samples for AFM

DNA templates A, B and C were obtained by restriction digestion with *Hin*dIII of plasmids pDE13, pSAP and pDSP, respectively. The DNA fragments containing the λ_{PR} promoter were gel purified in 1% agarose and electroeluted by means of an Elutrap apparatus (Schleicher & Schuell, Keene NH). The DNA was phenol/chloroform extracted, ethanol precipitated and resuspended in TE buffer (50 mM Tris–HCl pH 7.4, 1 mM EDTA). The DNA concentration was determined by absorbance measurements at 260 nm. *Escherichia coli* RNAP with a histidine tag in the β′ subunit was purified as described in Kashlev *et al*. (1993).

Open promoter complexes were obtained by mixing 200 fmol of DNA template and 200 fmol of RNAP in 10 µl of transcription buffer (20 mM Tris–HCl pH 7.9, 50 mM KCl, 5 mM $MgCl_2$, 10 mM dithiothreitol). The reaction was incubated for 15 min at 37°C. When present, $NiSO_4$ to a final concentration of 5 or 15 mM was added.

RNAP–DNA complexes in the presence of heparin were prepared as follows: RNAP stock solution was first incubated with 70 µg/ml heparin for 10 min. Then 10 fmol of DNA template B and 40 fmol of RNAP pre-incubated with heparin were added in 15 µl of deposition buffer containing heparin (4 mM HEPES pH 7.4, 10 mM NaCl, 2 mM $MgCl_2$, 70 µg/ml heparin). The reaction was incubated for 15 min at 37°C.

In vitro transcription

pSAP plasmid (170 fmol) harboring a λ_{PR} promoter was incubated with 600 fmol of His_6-tagged *E.coli* RNAP holoenzyme in 10 µl of either transcription buffer or deposition buffer. After 15 min incubation at 37°C, heparin, to a final concentration of 200 µg/ml, was added. When present, $NiSO_4$ to a final concentration of 5 or 10 mM was added. The reactions were incubated for 10 min at room temperature. Then 2 mM [α-^{32}P]UTP (800 Ci/mmol) (Amersham Pharmacia Biotech) and a mixture of 20 mM ATP, 20 mM GTP and 10 mM UTP were added and the reactions were incubated for 15 min at room temperature. Up to position 71, no cytosines are present in the coding strand, therefore, under these conditions, a 70 bp transcript is produced. Reactions were stopped by addition of a 30 µl solution containing 80% formamide, 2 mM EDTA, 0.1% xylene cyanol, 0.1% bromophenol blue. RNA transcript was analyzed by denaturing PAGE and visualized by autoradiography.

Gel mobility assay

DNA fragments of 350 bp were obtained from plasmids pDE13 (A) and pSAP (B) by PCR amplification using Deep Vent DNA polymerase (New England Biolabs). 'Middle' DNA fragments had the transcription start site located at 175 bp from the 5′ end, whereas 'end' DNA fragments had the transcription start site located at 318 bp from the 5′ end. All DNA fragments were gel purified and labeled at the 5′ end with [γ-^{32}P]ATP using T4 polynucleotide kinase (New England Biolabs).

Open promoter complexes were prepared in transcription buffer as described above using 40 fmol of DNA and 100 fmol of RNAP. The samples were loaded into a 4% (37.5:1 acrylamide/bis-acrylamide) non-denaturing polyacrylamide gel. Electrophoresis was carried out in TBE buffer at a constant voltage of 300 V for 10 h. The gel temperature was 11°C. Gel mobility analysis of DNA fragments without polymerase was performed under the same conditions with an electrophoresis time of 4 h. The bend angle calibration curve was determined in identical gel conditions with an electrophoresis time of 5 h. Bend angle markers were obtained from plasmids pJT170-3 through pJT170-6 as described in Thompson and Landy (1988). In all cases, migration of the complexes was visualized by autoradiography.

Atomic force microscopy

DNA samples were diluted to a concentration of 1–2 nM in 20 µl of deposition buffer (4 mM HEPES pH 7.4, 10 mM NaCl, 2 mM $MgCl_2$) and deposited onto freshly cleaved ruby mica (Mica New York, NY). After ~2 min, the mica disk was rinsed with water and dried with a weak flux of nitrogen. Complexes in the presence or absence of $NiSO_4$ were deposited as follows: 2 µl of the reaction were diluted in 18 µl of deposition buffer and immediately deposited onto freshly cleaved mica. After ~2 min, the mica disk was rinsed with <5 ml water and dried with nitrogen. RNAP–DNA complexes in the presence of heparin were deposited without further dilution, rinsed with water and dried with nitrogen. AFM images were obtained in air with a Nanoscope III microscope (Digital Instruments Inc., Santa Barbara, CA) operating in the tapping mode. All operations were done at room temperature. Commercial diving board silicon tips (Nanosensor, Digital Instruments) were used. The microscope was equipped with a type E scanner (12×12 µm). Images (512×512 pixels) were collected with a scan size of 2 µm at a scan rate of 2–5 scan lines/s. Water was purified in a Nanopure water purification apparatus (Barnstead, Dubuque IA). A detailed description of the sample preparation and AFM procedures can be found in C.Rivetti, M.Guthold and C.Bustamante (submitted).

Image analysis: DNA bend angle and contour length measurements

The AFM images were analyzed using locally written software (Alex). Measurements were performed only on those molecules that were completely visible in the image, that did not have any RNAP bound at the ends and molecules in which the shape was not ambiguous. The DNA path was digitized as previously described (Rivetti *et al*., 1996). The position of the center of the RNAP was selected manually and adjusted automatically at the nearest point on the traced contour line. DNA bend angle measurements with the tangents method were obtained by drawing lines from the center of the polymerase to the entry and exit points of the DNA. The deviation from linearity of one tangent with respect to the other corresponds to the bend angle. The direction of bending was obtained by taking the short arm (upstream DNA) as reference and determining whether the long arm (downstream DNA) deviated towards the left or towards the right.

The mean square end-to-end distance method relies on the fact that the average end-to-end distance of DNA molecules with a bend located at any position along the contour is smaller compared with that of unbent molecules. Using polymer chain statistics methods, it is possible to infer the DNA bend angle from the mean square end-to-end distance of a homogenous population of bent molecules (Rivetti *et al*., 1998). According to Equation 13 in Rivetti *et al*. (1998), the bend angle cosine of a worm-like chain at thermal equilibrium in two dimensions is given by:

$$\cos\beta = \frac{\langle R^2\rangle - 4PL + 8P^2(1 - e^{-l/2P}) + 8P^2(1 - e^{-(L-l)/2P})}{8P^2(1 - e^{-l/2P})\,(1 - e^{-(L-l)/2P})} \qquad (1)$$

where $\langle R^2\rangle$ is the mean square end-to-end distance obtained by averaging

the square of the end-to-end distances of each complex. *L* is the DNA contour length given by the mean of the Gaussian fitting to the contour length distribution (Table III). *l* and (*L* – *l*) are the contour lengths of the DNA arms and represent the position of the bend along the molecule. *l* was calculated from the mean contour length and from the mean arm ratio (Table I). *P* is the DNA persistence length which was assumed to be 53 nm as determined from DNA molecules imaged by AFM in similar conditions (Rivetti *et al*., 1996).

Images of artificial complexes were generated by superimposing the globular feature of an RNAP onto DNA molecules of images obtained with template C alone. This operation was performed with the 'copy and paste' function of the Alex software.

Acknowledgements

We thank Eric Sheagley for help with the gel mobility analysis, and S.Ottonello, G.Dieci and K.Rippe for critical reading and comments on the manuscript. C.R. was supported by EMBO and HFSP long-term fellowships. We are also grateful to the Institute of Molecular Biology at the University of Oregon, where most of the work has been carried out. This work was supported by grants from the National Institutes of Health (GM-32543) and the National Science Foundation (MBC 9118482 and DBI 9732140).

References

Amouyal,M. and Buc,H. (1987) Topological unwinding of strong and weak promoters by RNA polymerase. A comparison between the lac wild-type and the UV5 sites of *Escherichia coli*. *J. Mol. Biol.*, **195**, 795–808.

Brodolin,K.L., Studitsky,V.M. and Mirzabekov,A.D. (1993) Conformational changes in *E.coli* RNA polymerase during promoter recognition. *Nucleic Acids Res.*, **21**, 5748–5753.

Bustamante,C. and Rivetti,C. (1996) Visualizing protein–nucleic acid interactions on a large scale with the scanning force microscope. *Annu. Rev. Biophys. Biomol. Struct*., **25**, 395–429.

Bustamante,C., Keller,D. and Yang,G. (1993) Scanning force microscopy of nucleic acids and nucleoprotein assemblies. *Curr. Opin. Struct. Biol*., **3**, 363–372.

Bustamante,C., Rivetti,C. and Keller,D.J. (1997) Scanning force microscopy under aqueous solution. *Curr. Opin. Struct. Biol*., **7**, 709–716.

Craig,M.L., Suh,W.C. and Record,M.T. (1995) HO· and DNase I probing of $E\sigma^{70}$ RNA polymerase–λ_{PR} promoter open complexes: Mg^{2+} binding and its structural consequences at the transcripition start site. *Biochemistry*, **34**, 15634–15632.

Darst,S.A., Kubalek,E.W. and Kornberg,R.D. (1989) Three-dimensional structure of *Escherichia coli* RNA polymerase holoenzyme determined by electron crystallography. *Nature*, **340**, 730–732.

Forget,D., Robert,F., Grondin,G., Burton,Z.F., Greenblatt,J. and Coulombe,B. (1997) RAP74 induces promoter contacts by RNA polymerase II upstream and downstream of a DNA bend centered on the TATA box. *Proc. Natl Acad. Sci. USA*, **94**, 7150–7155.

Frontali,C., Dore,E., Ferrauto,A., Gratton,E., Bettini,A., Porzzan,M.R. and Valdevit,E. (1979) An absolute method for the determination of the persistence length of native DNA from electron micrographs. *Biopolymers*, **18**, 1353–1373.

Hansma,H.G., Laney,D.E., Bezanilla,M., Sinsheimer,R.L. and Hansma, P.K. (1995) Applications for atomic force microscopy of DNA. *Biophys. J.*, **68**, 1672–1677.

Hansma,H.G., Laney,D.E., Revenko,I., Kim,K. and Cleveland,J.P. (1996) Bending and motion of DNA in the atomic force microscope. In Sarma,R.H. and Sarma,M.H. (eds), *Biological Structure and Dynamics*. Adenine Press, Albany, NY pp. 249–257.

Hansma,H.G., Bezanilla,M., Nudler,E., Hansma,P.K., Hoh,J., Kashlev,M., Firouz,N. and Smith,B. (1997) Left-handed conformation of histidine-tagged RNA polymerase complexes imaged by atomic force microscopy. *Probe Microsc*., **1**, 127–143.

Hawley,D.K. and McClure,W.R. (1983) Compilation and analysis of *Escherichia coli* promoter DNA sequences. *Nucleic Acids Res.*, **11**, 2237–2255.

Hayes,J.J., Tullius,T.D. and Wolffe,A.P. (1990) The structure of DNA in a nucleosome. *Proc. Natl Acad. Sci. USA*, **87**, 7405–7409.

Heumann,H., Lederer,H., Baer,G., May,R.P., Kjems,J.K. and Crespi,H.L. (1988a) Spatial arrangement of DNA-dependent RNA polymerase of *Escherichia coli* and DNA in the specific complex. A neutron small angle scattering study. *J. Mol. Biol.*, **201**, 115–125.

Heumann,H., Ricchetti,M. and Werel,W. (1988b) DNA-dependent RNA polymerase of *Escherichia coli* induces bending or an increased flexibility of DNA by specific complex formation. *EMBO J.*, **7**, 4379–4381.

Kadesch,T.R., Williams,R.C. and Chamberlin,M.J. (1980) Electron microscopic studies of the binding of *Escherichia coli* RNA polymerase to DNA. I. Characterization of the non-specific interactions of holoenzyme with a restriction fragment of bacteriophage T7 DNA. *J. Mol. Biol.*, **136**, 65–78.

Kasas,S. *et al*. (1997) *Escherichia coli* RNA polymerase activity observed using atomic force microscopy. *Biochemistry*, **36**, 461–468.

Kashlev,M., Martin,E., Polyakov,A., Severinov,K., Nikiforov,V. and Goldfarb,A. (1993) Histidine-tagged RNA polymerase: dissection of the transcription cycle using immobilized enzyme. *Gene*, **130**, 9–14.

Kim,T.-K., Lagrange,T., Wang,Y.-H., Griffith,J.D., Reinberg,D. and Ebright,R.H. (1997) Trajectory of DNA in the RNA polymerase II transcription preinitiation complex. *Proc. Natl Acad. Sci. USA*, **94**, 12268–12273.

Kuhnke,G., Theres,C., Fritz,H.J. and Ehring,R. (1989) RNA polymerase and *gal* repressor bind simultaneously and with DNA bending to the control region of the *Escherichia coli* galactose operon. *EMBO J*., **8**, 1247–1255.

Landau,L.D. and Lifschitz,E.M. (1980) *Fluctuations in the Curvature of Long Molecules. Statistical Physics Part I*. Pergamon Press, Oxford.

Landau,L.D. and Lifshitz,E.M. (1986) *Statistical Physics part I*. Pergamon Press, Oxford, UK.

Leirmo,S. and Record,M.T. (1990) *Structural, Thermodynamic and Kinetic Studies of the Interaction of Escherichia coli σ70 RNA Polymerase with Promoter DNA*. Springer-Verlag, New York, NY.

Meyer-Alme,F.J., Heumann,H. and Porschke,D. (1994) The structure of the RNA polymerase–promoter complex: DNA bending by quantitative electrooptics. *J. Mol. Biol.*, **236**, 1–6.

Nickerson,C.A. and Achberger,E.C. (1995) Role of curved DNA in binding of *Escherichia coli* RNA polymerase to promoters. *J. Bacteriol*., **177**, 5756–5761.

Niyogi,S.K. and Feldman,R.P. (1981) Effect of several metal ions on misincorporation during transcription. *Nucleic Acids Res*., **9**, 2615–2627.

Polyakov,A., Severinova,E. and Darst,S.A. (1995) Three-dimensional structure of *E.coli* core RNA polymerase: promoter binding and elongation conformation of the enzyme. *Cell*, **83**, 365–373.

Rees,W.A., Keller,R.W., Vesenka,J.P., Yang,G. and Bustamante,C. (1993) Evidence of DNA bending in transcription complexes imaged by scanning force microscopy. *Science*, **260**, 1646–1649.

Rippe,K., Guthold,M., von Hippel,P.H. and Bustamante,C. (1997) Transcriptional activation via DNA-looping: visualization of intermediates in the activation pathway of *E.coli* RNA polymerase-σ54 holoenzyme by scanning force microscopy. *J. Mol. Biol.*, **270**, 125–138.

Rivetti,C., Guthold,M. and Bustamante,C. (1996) Scanning force microscopy of DNA deposited on mica: equilibration versus kinetic trapping studied by polymer chain analysis. *J. Mol. Biol.*, **264**, 919–932.

Rivetti,C., Walker,C. and Bustamante,C. (1998) Polymer chain statistics and conformational analysis of DNA molecules with bends or sections of different flexibility. *J. Mol. Biol.*, **280**, 41–59.

Robert,F., Douziech,M., Forget,D., Egly,J.M., Greenblatt,J., Burton,Z.F. and Coulombe,B. (1998) Wrapping of promoter DNA around the RNA polymerase II initiation complex induced by TFIIF. *Mol. Cell*, **2**, 341–351.

Roe,J.H., Burgess,R.R. and Record,M.T.,Jr (1985) Temperature dependence of the rate constants of the *Escherichia coli* RNA polymerase λ_{PR} promoter interaction. Assignment of the kinetic steps corresponding to protein conformational change and DNA opening. *J. Mol. Biol.*, **184**, 441–453.

Ross,W., Gosink,K.K., Salomon,J., Igarashi,K., Zou,C., Ishihama,A., Severinov,K. and Gourse,R.L. (1993) A third recognition element in bacterial promoters: DNA binding by the α subunit of RNA polymerase. *Science*, **262**, 1407–1412.

Schickor,P., Metzger,W., Werel,W., Lederer,H. and Heumann,H. (1990) Topography of intermediates in transcription initiation of *E.coli*. *EMBO J.*, **9**, 2215–2220.

Schlax,P.J., Capp,M.W. and Record,M.T. (1995) Inhibition of transcription initiation by *lac* repressor. *J. Mol. Biol.*, **245**, 331–350.

Schulz,A., Mucke,N., Langowski,J. and Rippe,K. (1998) Scanning force

microscopy of *Escherichia coli* RNA polymerase·σ^{54} holoenzyme complexes with DNA in buffer and in air. *J. Mol. Biol.*, **283**, 821–836.
Shu,W.C. and Record,M.T. (1993) Two open complexes and a requirement for Mg^{2+} to open the λ_{PR} transcription start site. *Science*, **259**, 358–361.
Thompson,J.F. and Landy,A. (1988) Empirical estimation of protein-induced DNA bending angles: applications to lambda site-specific recombination complexes. *Nucleic Acids Res.*, **16**, 9687–9705.
Tsodikov,O.V., Craig,M.L., Saecker,R.M. and Record,M.T. (1998) Quantitative analysis of multiple-hit footprinting studies to characterize DNA conformational changes in protein–DNA complexes: application to DNA opening by Eσ^{70} polymerase. *J. Mol. Biol.*, **283**, 757–769.
von Hippel,P.H., Bear,D.G., Morgan,W.D. and McSwiggen,J.A. (1984) Protein–nucleic acid interactions in transcription. *Annu. Rev. Biochem.*, **53**, 389–446.
Wasserman,S.A., White,J.H. and Cozzarelli,N.R. (1988) The helical repeat of double-stranded DNA varies as a function of catenation and supercoiling. *Nature*, **334**, 448–450.
Williams,R.C. and Chamberlin,M.J. (1977) Electron microscope studies of transient complexes formed between *Escherichia coli* RNA polymerase holoenzyme and T7 DNA. *Proc. Natl Acad. Sci. USA*, **74**, 3740–3744.

Received March 17, 1999; revised and accepted June 21, 1999